IET Communications

Research Article

IET Journals
The Institution of Engineering and Technology

Multicarrier modulation with variable peak-to-average power ratio using partial fast Fourier transform

ISSN 1751-8628
Received on 25th November 2014
Revised on 18th February 2015
Accepted on 14th March 2015
doi: 10.1049/iet-com.2014.1086
www.ietdl.org

Himanshu Nayar[1], *Vinay J. Ribeiro*[2] ✉, *Ranjan K. Mallik*[3]

[1]Department of Electrical Engineering and Computer Science, University of Michigan, Ann Arbor, MI 48109, USA
[2]Department of Computer Science and Engineering, Indian Institute of Technology Delhi, Hauz Khas, New Delhi 110016, India
[3]Department of Electrical Engineering, Indian Institute of Technology Delhi, Hauz Khas, New Delhi 110016, India
✉ E-mail: vinay@iitd.ac.in

Abstract: The authors present a novel frequency division multiplexing scheme which can generate a signal whose worst-case peak-to-average power ratio (PAPR) is tunable by an input parameter; they call this scheme tunable PAPR frequency division multiplexing (TP-FDM). Special cases of TP-FDM are orthogonal FDM (OFDM) and single carrier (SC) modulation. Unlike several other proposed PAPR reduction schemes, TP-FDM requires no per-symbol side information to be sent from transmitter to receiver. TP-FDM has overall computational requirements almost the same as OFDM. The author's study of the symbol error rate (SER) of TP-FDM in a Rayleigh fading channel shows that higher PAPR signals give a better SER performance. Thus, instead of choosing either of the extremes, OFDM and SC modulation, as is currently done in some cellular systems, one can tune the PAPR with TP-FDM to the maximum suitable for the transmitter and receiver device electronics, so as to minimise SER. They compare and contrast TP-FDM with transform precoded OFDM methods in terms of SER and PAPR. They also extend TP-FDM to a multi-user scenario.

1 Introduction

The problem of peak-to-average power ratio (PAPR) in communication systems using orthogonal frequency division multiplexing (OFDM) is well known. Given a set of input constellation points $X = [X_0, X_1, \ldots, X_{N-1}]$, the baseband OFDM signal $s[n]$ in the discrete-time domain is given by

$$s[n] = \frac{1}{\sqrt{N}} \sum_{l=0}^{N-1} X_l e^{j2\pi nl/N}; \quad n = 0, 1, \ldots, N-1 \tag{1}$$

The PAPR of $s[n]$, $\rho(s)$, is defined as the ratio of the peak power to the average power of the signal, and is given by

$$\rho(s) := \frac{\max_{0 \le n \le N-1} |s[n]|^2}{(1/N) \sum_{n=0}^{N-1} |s[n]|^2} \tag{2}$$

The worst-case PAPR of an arbitrary OFDM signal is N. Large PAPR is known to negatively affect system performance [1], and necessitates the use of high power amplifiers with large linear range and complex digital-to-analogue converters (DACs). A cyclic prefix is typically attached to an OFDM signal in order to simplify channel estimation and equalisation [2].

Several PAPR reduction techniques have been proposed which can be broadly classified into six categories: (i) transform precoded OFDM, (ii) clipping and filtering, (iii) coding schemes, (iv) phase modification methods, (v) non-linear companding transforms and (vi) tone reservation (TR) and tone injection (TI) [1, 3]. Our scheme resembles those in the first category and differs qualitatively from the other five. Each of the last five methods performs one of the following, none of which are required by our scheme: distortion of a pre-existing OFDM signal, introduction of redundant bits, transmission of side information to the receiver, solving an optimisation problem at the transmitter or the receiver. It is hence infeasible to make a purely quantitative comparison of our scheme with these schemes. A quantitative comparison of symbol error rate (SER) and PAPR with transform precoded OFDM schemes is made in Sections 4.1 and 4.2, respectively.

We describe each of these categories briefly below and highlight the differences of our solution with these techniques:

1. Transform precoded OFDM: Here data symbols are first sent through a transform, such as a discrete Hartley transform (DHT) [4], a Walsh–Hadamard transform (WHT) [5] or a discrete Fourier transform (DFT) [6, 7]. The resulting transformed symbol vector is now fed to an OFDM transmitter.

Note that DFT-precoded OFDM is nothing but single carrier (SC) modulation which certain advanced communications systems [such as 4G long-term evolution (LTE)] use on the uplink [6, 7]. Service providers can afford to use expensive electronics at the base-station which can tolerate a high PAPR and hence employ OFDM, whereas this is not the case for client handsets which are designed to be low cost. A single-carrier modulated signal $s[n]$ in the discrete-time domain is given by

$$s[n] = X_n; \ n = 0, 1, \ldots, N-1 \tag{3}$$

It is clear that SC modulated signals have a PAPR of 1 if all constellation points X_n are of the same magnitude. However, the SER of SC modulated signals can be worse than OFDM in frequency selective fading channels in certain situations [8].

We present a novel scheme called tunable PAPR frequency division multiplexing (TP-FDM), which through a parameter k (which must be a factor of N), can adjust the worst-case PAPR of the generated signal to N/k. OFDM ($k = 1$) and SC modulation ($k = N$) are two extremes of TP-FDM.

In choosing the parameter k, there is a tradeoff between achieving smaller PAPR and achieving lower SER. Clearly, higher values of k provide smaller PAPR, but, as our results for Rayleigh fading channels show, also leads to poorer SER performance. For communication systems using TP-FDM, the parameter k must hence be chosen to minimise SER, under the constraint that the communications electronics can tolerate the resulting PAPR.

2. Clipping and filtering: High peaks of the signal are clipped at the transmitter to remove peaks in the signal [9–12]. This leads to

IET Commun., 2015, Vol. 9, Iss. 12, pp. 1450–1457

in-band distortion and out-of-band radiation. The out-of-band radiation can be removed by filtering the signal before transmission which, in turn, may increase PAPR. The location of the clipping(s) must be estimated at the receiver. Our scheme introduces no in-band distortion and does not need to estimate unknown clipping point locations.

3. Coding schemes: These add extra or redundant bits to the data, that is, code the data, so that the resultant generated signals do not have high PAPR [13–15]. Essentially, certain bit combinations which give rise to high PAPR are never transmitted. Introducing the redundant bits reduces the effective data throughput. Our scheme does not introduce any redundant bits.

4. Phase modification methods: Partial transmission sequence (PTS), selective mapping and sign adjustment are three methods in by which the phase of various sub-carriers are modified to reduce PAPR.

PTS divides the N-symbol input vector into J blocks, each of size N [16]. Each block essentially consists of a subset of symbols and zeroes. The sum of all blocks gives the original vector. PTS takes the N-point inverse fast Fourier transform (IFFT) of each block, phase shifts each by some amount and adds the resultant up. The goal is to find the set of phase shifts which minimise PAPR. PTS needs J different N-point IFFT computations, performs an optimisation to find the best phase factors, and transmits the optimal phase factors as side information.

SLM takes the input symbol vector, applies different phase vectors to it, determines the best PAPR reducing phase vector, and transmits the time signal obtained after taking the IFFT [17]. SLM needs to communicate as side-information the particular choice of phase vector to the receiver for each OFDM symbol.

Sign adjustment schemes adjust the sign of each subcarrier to reduce the PAPR [18, 19]. As the signs of subcarriers contain no information, there is a corresponding decrease in rate of each of these schemes. The transmitter determines the optimum set of signs by solving a combinatorial optimisation problem. The receiver ignores the signs of all subcarriers as they contain no information.

5. Nonlinear companding transforms: Companding distorts the amplitude of an input signal in a predefined manner to enlarge signals with small amplitude and compress signals with large amplitude [20]. The receiver applies the inverse of the companding operation. In doing so, it, however, may amplify channel distortions and noise, resulting in a phenomenon called companding noise. Filtering and iterative algorithms can be used to remove the effect of companding noise. Our scheme does not perform companding and is a purely digital domain solution.

6. TR and TI: In TR, some subcarriers are reserved for PAPR reduction signals. The rest of the subcarriers are used for data transmission. TR uses convex optimisation to find the best PAPR reducing signal using the reserved subset of tones. Our method does not require some subcarriers to be used specially for PAPR reduction.

TI extends the used constellations such that each input data vector can correspond to multiple constellation points [21]. This method chooses the optimal set of constellation points to reduce the PAPR. TI methods require optimisation to be carried out and also use larger transmit power than conventional OFDM because of the redundant constellation points.

The salient features of our proposed modulation scheme TP-FDM are:

1. It allows the PAPR to be adjusted through a parameter k.
2. It requires no side information, unlike certain other PAPR reduction schemes [16, 17]. The parameter k can be pre-negotiated between the transmitter and receiver and kept constant thereafter.
3. Each subcarrier in TP-FDM contains information about k different data constellation points. Thus, TP-FDM has the property of k-symbol decodability.
4. The additional computational cost (sum of computations at transmitter and receiver) of TP-FDM over OFDM is only $O(N)$. TP-FDM has added complexity at the receiver, which is offset by reduced complexity at the transmitter, when compared to conventional OFDM.
5. It can be used in multi-user scenarios and not just for point-to-point communications. We term the multi-user implementation of TP-FDM as tunable PAPR frequency division multiple access (TP-FDMA).

This paper is organised as follows. Preliminaries are given in Section 2. Section 3 presents TP-FDM for a single transmitter–receiver pair; its performance is analysed in Section 4. Section 5 extends TP-FDM to the multi-user case. Section 6 gives some concluding remarks.

2 Preliminaries

Typical fast Fourier transform (FFT) algorithms, such as Cooley–Tukey, are implemented recursively in multiple steps, where each step consists of a number of smaller sized FFTs. TP-FDM essentially implements an FFT algorithm partially, that is, it terminates an FFT algorithm at an intermediate step. Although a partial implementation of an FFT has been earlier used to generate or decode a subset of subcarriers for a standard OFDM signal [22], to the best of our knowledge, we are the first to use a partial implementation of an FFT to generate a new modulation scheme to control the PAPR.

Consider a signal $c[n]$ and its DFT $C[m]$; $m, n = 0, \ldots, N-1$. We assume that parameter k is a factor of N. We map indices n and m to two dimensions via

$$\begin{aligned} n &= n_1 + kn_2 \\ \text{where } n_1 &= 0, \ldots, k-1 \text{ and } n_2 = 0, \ldots, (N/k)-1 \end{aligned} \tag{4}$$

and

$$\begin{aligned} m &= (N/k)m_1 + m_2 \\ \text{where } m_1 &= 0, \ldots, k-1 \text{ and } m_2 = 0, \ldots, (N/k)-1 \end{aligned} \tag{5}$$

We use the notation $c[n_1, n_2]$ and $c[n]$ interchangeably below. Similarly $C[m_1, m_2]$ and $C[m]$ are used interchangeably.

Define W_N as $W_N := \mathrm{e}^{-\mathrm{j}2\pi/N}$. Then we have

$$\begin{aligned} C[m_1, m_2] &= \frac{1}{\sqrt{N}} \sum_{n_1} \sum_{n_2} c[n_1, n_2] \times W_N^{((N/k)m_1+m_2)(n_1+kn_2)} \\ &= \frac{1}{\sqrt{N}} \sum_{n_1} \left(\sum_{n_2} c[n_1, n_2] \times W_{N/k}^{m_2 n_2} \right) W_N^{m_2 n_1} W_k^{m_1 n_1} \end{aligned} \tag{6}$$

Note that we employ unitary DFT and inverse DFT (IDFT) definitions in this paper.

Essentially the N-length FFT can be computed in the following steps: (i) populate a $k \times N/k$ matrix column-wise with elements of $c[n]$, (ii) replace each row by its length-N/k FFT, (iii) multiply the element in position (n_1, m_2) by the twiddle factor $W_N^{m_2 n_1}$, (iv) replace each column with its length-k FFT and (v) read out elements of the matrix row wise [23].

Define $\boldsymbol{P}_u$, where u is a factor of N, as the permutation matrix which transforms vector $\boldsymbol{x} = [x_0, x_1, \ldots, x_{N-1}]^{\mathrm{T}}$ into $[x_0, x_u, x_{2u}, \ldots, x_1, x_{1+u}, x_{1+2u}, \ldots]^{\mathrm{T}}$. Also define $\boldsymbol{B}_u$ as $\boldsymbol{B}_u := \boldsymbol{I}_{N/u} \otimes \boldsymbol{G}_u$ where $\boldsymbol{I}_u$ is the $u \times u$ identity matrix, $\boldsymbol{G}_u$ is the u-point DFT matrix and $\otimes$ denotes the Kronecker product of matrices.

Let $\boldsymbol{D}_{N/k}$ be a diagonal matrix whose lth diagonal entry is the twiddle factor $W_N^{l_1 l_2}$ where $l_1 = l \text{ div}(N/k)$ and $l_2 = l \bmod (N/k)$. Here div and mod are the division and modulo operators for integer arithmetic which result in the quotient and the remainder, respectively. Note that each diagonal entry of $\boldsymbol{D}_{N/k}$ has magnitude 1. It is easily shown that $D_1 = D_N = \boldsymbol{I}_N$. Equivalent to (6), the

N-point DFT matrix $\boldsymbol{G}_N$ can then be represented as

$$\boldsymbol{G}_N = \boldsymbol{P}_k \boldsymbol{B}_k \boldsymbol{P}_{N/k} \boldsymbol{D}_{N/k} \boldsymbol{B}_{N/k} \boldsymbol{P}_k \tag{7}$$

Consequently, the N-point IDFT matrix is

$$\begin{aligned} \boldsymbol{G}_N^{-1} &= \boldsymbol{G}_N^{\mathrm{H}} \\ &= \boldsymbol{P}_k^{\mathrm{H}} \boldsymbol{B}_{N/k}^{\mathrm{H}} \boldsymbol{D}_{N/k}^{\mathrm{H}} \boldsymbol{P}_{N/k}^{\mathrm{H}} \boldsymbol{B}_k^{\mathrm{H}} \boldsymbol{P}_k^{\mathrm{H}} \\ &= \boldsymbol{P}_{N/k} \boldsymbol{B}_{N/k}^{\mathrm{H}} \boldsymbol{D}_{N/k}^{\mathrm{H}} \boldsymbol{P}_k \boldsymbol{B}_k^{\mathrm{H}} \boldsymbol{P}_{N/k} \end{aligned} \tag{8}$$

since $\boldsymbol{P}_k^{\mathrm{H}} = \boldsymbol{P}_k^{\mathrm{T}} = \boldsymbol{P}_{N/k}$, where $(\cdot)^{\mathrm{T}}$ denotes the transpose operator and $(\cdot)^{\mathrm{H}}$ denotes the Hermitian (conjugate transpose) operator.

3 TP-FDM for single transmitter–receiver pair

We now describe TP-FDM for a single transmitter and receiver pair. We will extend TP-FDM to a multiple user scenario in Section 5.

3.1 Transmitter

Consider the TP-FDM transmitter communication block diagram depicted in Fig. 1*a*. The input bits corresponding to a single OFDM symbol are first mapped to constellation points $\boldsymbol{X} = [X_0, \ldots, X_{N-1}]^{\mathrm{T}}$. We then perform the following operations on $\boldsymbol{X}$:

1. Partition the N-symbol transmission vector of constellation points into k equal partitions. We use the notation $\boldsymbol{X}^{(i)}$ to represent the ith partition $[X_{iN/k}, X_{iN/k+1}, \ldots, X_{(i+1)N/k-1}]^{\mathrm{T}}$.
2. Perform an IFFT of size N/k individually on each of these partitions.
3. Form a new vector by placing in it the first elements of the resultant IFFT vectors in a round-robin fashion, continuing likewise with their second elements and so on. We call this operation an 'interleaving union'.

After appending a cyclic prefix, we have the time samples of the baseband TP-FDM signal. These are then converted to an analogue signal using DACs and then up-converted to the passband.

It is easy to see that $k = 1$ corresponds to OFDM and $k = N$ corresponds to SC modulation.

Equivalently, TP-FDM generates the baseband time-domain signal y (prior to appending a cyclic prefix) through

$$\boldsymbol{y} = \boldsymbol{P}_{N/k} \boldsymbol{B}_{N/k}^{\mathrm{H}} \boldsymbol{X} \tag{9}$$

We denote the DFT of $\boldsymbol{y}$ by $\boldsymbol{Y} := \boldsymbol{G}_N \boldsymbol{y}$ hereafter.

3.2 Receiver

We now describe the structure of the TP-FDM receiver depicted in Fig. 1*b*. If we feed in the received TP-FDM signal into this receiver, then the output of the equaliser, $\hat{\boldsymbol{Y}}$, is an estimate of $\boldsymbol{Y}$.

From $\hat{\boldsymbol{Y}}$ we obtain estimates of constellation points X as given by

$$\hat{\boldsymbol{X}} = \boldsymbol{D}_{N/k}^{\mathrm{H}} \boldsymbol{P}_{N/k}^{\mathrm{H}} \boldsymbol{B}_k^{\mathrm{H}} \boldsymbol{P}_k^{\mathrm{H}} \hat{\boldsymbol{Y}} = \boldsymbol{D}_{N/k}^{\mathrm{H}} \boldsymbol{P}_k \boldsymbol{B}_k^{\mathrm{H}} \boldsymbol{P}_{N/k} \hat{\boldsymbol{Y}} \tag{10}$$

Equivalently, the following operations implement (10):

1. Partition $\hat{\boldsymbol{Y}}$ into N/k partitions, each of size k, such that the ith partition (for $i = 0, 1, \ldots, N/k - 1$) is $[\hat{Y}_i, \hat{Y}_{i+N/k}, \ldots, \hat{Y}_{i+(k-1)N/k}]^{\mathrm{T}}$. We refer to this operation as 'interleaved partitioning'.
2. Length-k IFFT of each partition.
3. Interleaved union of partitions.
4. Multiplication of the resultant by diagonal matrix $\boldsymbol{D}_{N/k}^{\mathrm{H}}$.

4 Performance analysis

We now compare TP-FDM with OFDM and certain transform precoded OFDM schemes in terms of SER for different channel models, PAPR, symbol decidability and computational requirements.

4.1 Symbol error rate

We study the SER for two channel models: (i) an AWGN channel with no fading, and (ii) a frequency selective Rayleigh fading channel with additive noise. We denote the DFT of the received signal as vector $\boldsymbol{Z} = [Z_0, Z_1, \ldots, Z_{N-1}]^{\mathrm{T}}$ and that of additive noise by $\boldsymbol{\eta} = [\eta_0, \eta_1, \ldots, \eta_{N-1}]^{\mathrm{T}}$. The vector $\boldsymbol{\eta}$ has elements which are

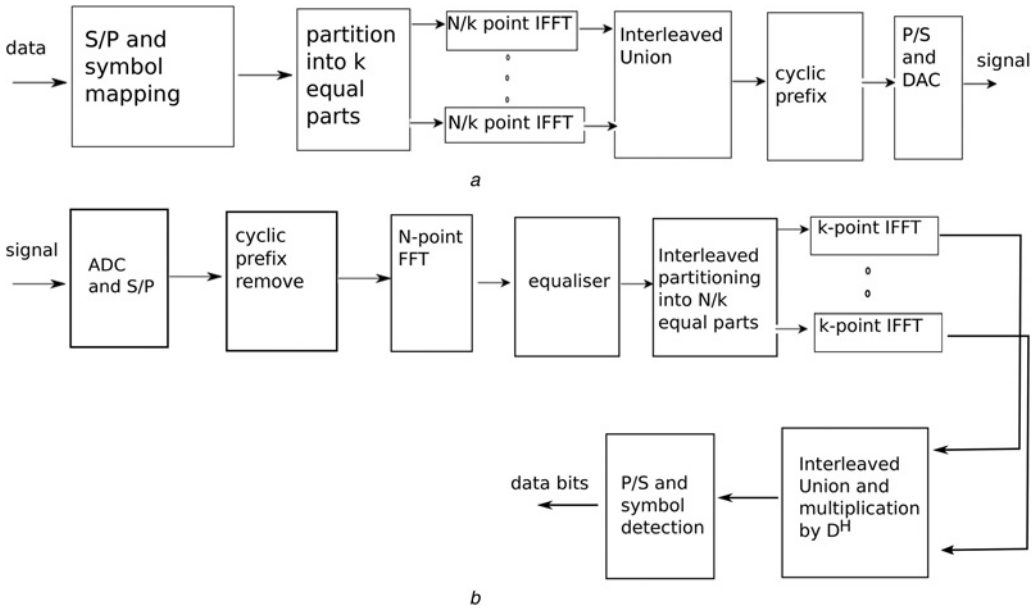

Fig. 1 *TP-FDM Block Diagrams*

a TP-FDM transmitter
b TP-FDM receiver

IET Commun., 2015, Vol. 9, Iss. 12, pp. 1450–1457

complex Gaussian, circularly symmetric and independent and identically distributed (i.i.d.).

4.1.1 Additive white Gaussian noise (AWGN) channel: For this channel model

$$\boldsymbol{Z} = \boldsymbol{Y} + \boldsymbol{\eta} \tag{11}$$

The estimates of constellation points are obtained as

$$\hat{\boldsymbol{X}} = \boldsymbol{D}_{N/k}^{\mathrm{H}} \boldsymbol{P}_k \boldsymbol{B}_k^{\mathrm{H}} \boldsymbol{P}_{N/k} (\boldsymbol{Y} + \boldsymbol{\eta}) = \boldsymbol{X} + \boldsymbol{D}_{N/k}^{\mathrm{H}} \boldsymbol{P}_k \boldsymbol{B}_k^{\mathrm{H}} \boldsymbol{P}_{N/k} \boldsymbol{\eta} \tag{12}$$

Multiplication of $\boldsymbol{\eta}$ by an FFT matrix retains the complex Gaussian, independent, and circularly symmetric probability distribution of the noise vector. The diagonal matrix $\boldsymbol{D}_{N/k}^{\mathrm{H}}$ only rotates the circularly symmetric probability distribution of different elements of the noise vector by different amounts. Thus, the distribution of the noise vector does not change after multiplication with $\boldsymbol{D}_{N/k}^{\mathrm{H}} \boldsymbol{P}_k \boldsymbol{B}_k^{\mathrm{H}} \boldsymbol{P}_{N/k}$. Consequently, the symbol error rates for any modulation scheme in TP-FDM are the same as that for OFDM.

Note that it has been proved that WHT-precoded OFDM gives the same SER performance as OFDM over an AWGN channel [5]. The proof for this result only relies on the fact that the basic functions of the WHT transform are orthogonal. The result, hence also holds for DHT-precoded OFDM too.

4.1.2 Frequency selective Rayleigh fading channel: In this section, we compare the SER performance, of TP-FDM with that of DHT-precoded OFDM [4], DFT-precoded OFDM (i.e. SC modulation) [6], WHT-precoded OFDM [5] and OFDM, over a frequency selective Rayleigh fading channel through simulations.

We consider a baseband signal of 20 MHz consisting of $N = 64$ subcarriers. The signal is oversampled by a factor of four and transmitted over a standard channel model `itur3GIAx`, in matlab. This channel is an ITU-R 3G frequency selective multipath Rayleigh channel (indoor Channel A), consisting of six paths. The received signal is equalised using a zero forcing equaliser, assuming perfect knowledge of the channel impulse response. For each set of parameters a total of 10 000 simulation runs were executed.

In Figs. 2*a* and *b*, we compare the SER performance for various schemes for quadrature phase shift keyed (QPSK) and quadrature amplitude modulator-64 (QAM-64) modulation over the multipath Rayleigh fading channel. Recall that DFT precoded OFDM and TP-FDM with parameter $k = 64$ are equivalent modulation schemes. Similarly OFDM and TP-FDM with parameter $k = 1$ are equivalent.

Observe that in all cases the SER of DHT, WHT and DFT precoded OFDM are almost the same. TP-FDM with decreasing values of k gives lower SER, and OFDM outperforms all schemes. Since TP-FDM with parameter k has k-symbol decodability, severe fading on a single subcarrier can cause errors in k data symbols. Thus, intuitively, in a frequency selective fading channel, one can expect TP-FDM with a smaller k gives a better SER performance than that of TP-FDM with a larger k.

4.1.3 PAPR analysis: We first use (9) to derive the following result regarding worst-case PAPR for TP-FDM. We then compute the complementary cumulative distribution function (CCDF) of PAPR for various schemes through simulations.

Theorem 1: Assuming that the average power of constellation points in all k partitions of symbols, that is $\boldsymbol{X}^{(i)}$ $\forall i$, is the same, the worst-case PAPR of a TP-FDM baseband signal $\boldsymbol{y}$ is N/k.

Proof: Consider

$$\bar{\boldsymbol{y}} := \boldsymbol{B}_{N/k}^{\mathrm{H}} \boldsymbol{X} \tag{13}$$

Comparing (9) and (13), we see that the PAPR of $\boldsymbol{y}$ and $\bar{\boldsymbol{y}}$ are the same, that is, $\rho(\boldsymbol{y}) = \rho(\bar{\boldsymbol{y}})$, since the permutation operation $\boldsymbol{P}_{N/k}$ preserves PAPR.

From (13), we observe that

$$\bar{\boldsymbol{y}}^{(i)} = \boldsymbol{G}_{N/k} \boldsymbol{X}^{(i)} \tag{14}$$

Since $\boldsymbol{G}_{N/k}$ is unitary, it follows that $\bar{\boldsymbol{y}}^{(i)}$ and $\boldsymbol{X}^{(i)}$ have the same average powers. Hence, from our assumption of equal power in $\boldsymbol{X}^{(i)}$ for all i, it follows that $\bar{\boldsymbol{y}}^{(i)}$, for all i, have same average power. This power equals $(1/N) \sum_{n=0}^{N-1} |\bar{y}[n]|^2$. Denote the set $\{iN/k, iN/k + 1, \ldots, (i+1) N/k - 1\}$ by κ_i. Thus

$$\begin{aligned} \rho(\bar{\boldsymbol{y}}) &= \frac{\max_{0 \le n \le N-1} |\bar{y}[n]|^2}{(1/N) \sum_{n=0}^{N-1} |\bar{y}[n]|^2} \\ &= \frac{\max_{0 \le i \le k-1} (\max_{n \in \kappa_i} |\bar{y}[n]|^2)}{(1/N) \sum_{n=0}^{N-1} |\bar{y}[n]|^2} \\ &= \max_{0 \le i \le k-1} \left(\frac{\max_{n \in \kappa_i} |\bar{y}[n]|^2)}{(k/N) \sum_{n \in \kappa_i} |\bar{y}[n]|^2} \right) \\ &= \max_{0 \le i \le k-1} \rho(\bar{\boldsymbol{y}}^{(i)}) \end{aligned} \tag{15}$$

The worst-case PAPR of the result of an N/k-point IFFT is N/k. This

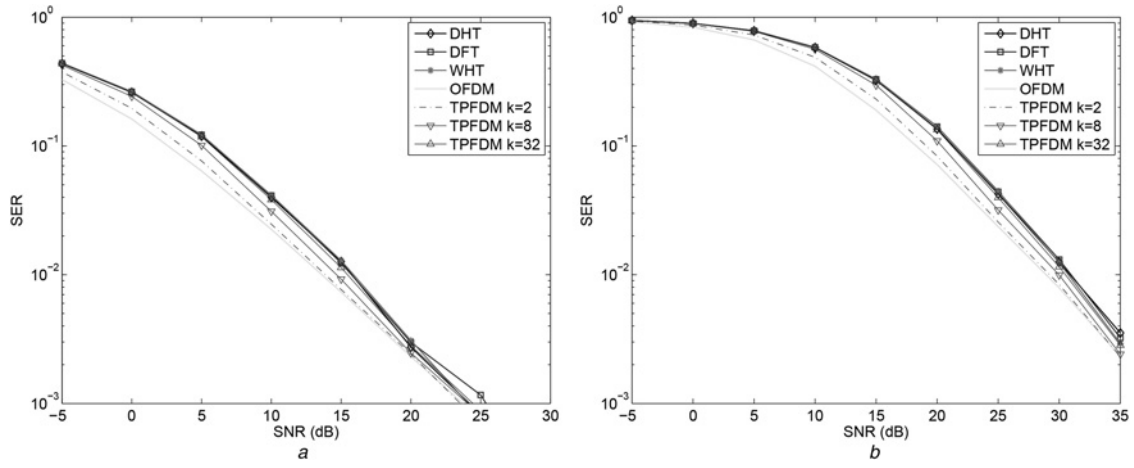

Fig. 2 *SER against SNR for various modulation schemes over a multipath Rayleigh fading channel*

a QPSK modulation

b QAM64 modulation

occurs when only one IFFT value is non-zero. Thus $\rho(\bar{\boldsymbol{y}}^{(i)})$, for any i, is in the worst case N/k. From (15), we conclude that the worst-case value of $\rho(\bar{\boldsymbol{y}})$ and hence the worst-case value of $\rho(\boldsymbol{y})$ is N/k. □

We now compare the PAPR for various modulation schemes, of TP-FDM with that of DHT-precoded OFDM, DFT-precoded OFDM (i.e. SC modulation), WHT-precoded OFDM and OFDM.

In Figs. 3*a* and *b*, we compare the CCDF of PAPR for the various schemes for QPSK and QAM-64 modulation. The CCDF of PAPR was obtained from 10 000 simulation runs using oversampled signals from all schemes. Observe that in all cases, the CCDF of PAPR for TP-FDM decreases with increasing k.

Hence, for TP-FDM, there is a clear trade-off between SER and PAPR. TP-FDM signals with larger PAPR signals give superior SER performance than signals with lower PAPR. From a practical perspective, a TP-FDM user must thus choose parameter k to minimise the SER, under the constraint that the transmitter electronics can tolerate the corresponding PAPR level, that is, it does not cause signal distortion because of the clipping or does not become too power inefficient.

Also observe that the CCDF of PAPR of DHT-precoded and WHT-precoded OFDM are clearly less than that of OFDM but larger than that of DFT-precoded OFDM, which corroborate the findings in [24].

4.1.4 k-Symbol decodability: In OFDM, each data symbol is mapped to one subcarrier. In TP-FDM, k different symbols are mapped to each subcarrier as we prove next.

Theorem 2: The complex amplitude of each subcarrier of the transmitted TP-FDM signal is a linear combination of exactly k symbols.

Proof: From (7) and (9), the transmitted baseband signal in the frequency domain is given by

$$\begin{aligned}\boldsymbol{Y} &= \boldsymbol{G}_N\boldsymbol{y}\\ &= \boldsymbol{P}_k\boldsymbol{B}_k\boldsymbol{P}_{N/k}\boldsymbol{D}_{N/k}\boldsymbol{B}_{N/k}\boldsymbol{P}_k\boldsymbol{P}_{N/k}\boldsymbol{B}_{N/k}^{\mathrm{H}}\boldsymbol{X}\\ &= \boldsymbol{P}_k\boldsymbol{B}_k\boldsymbol{P}_{N/k}\boldsymbol{D}_{N/k}\boldsymbol{X}\end{aligned} \tag{16}$$

since $\boldsymbol{P}_k\boldsymbol{P}_{N/k} = \boldsymbol{I}_N = \boldsymbol{B}_{N/k}\boldsymbol{B}_{N/k}^{\mathrm{H}}$. Since $\boldsymbol{D}_{N/k}$ is a diagonal matrix consisting of twiddle factors and $\boldsymbol{P}_{N/k}$ only permutes entries of any vector it multiplies, we conclude that each element of the vector $\boldsymbol{P}_{N/k}\boldsymbol{D}_{N/k}\boldsymbol{X}$ is a product of one element of $\boldsymbol{X}$ and some twiddle factor. Since each row in $\boldsymbol{B}_k$ has k non-zero entries, it follows that each element of $\boldsymbol{Y}$ is a linear combination of k elements of $\boldsymbol{X}$. □

4.2 Computational comparison of OFDM with TP-FDM

Let us compute the reduction in complex multiplications at the TP-FDM transmitter compared to conventional OFDM which uses a Cooley–Tukey FFT implementation. Recall that the number of multiplications and the number of additions of a radix-2 Cooley–Tukey N-point FFT are $(N/2)\log_2 N$ and $N\log_2 N$, respectively [23].

The number of complex multiplications, $M_{\mathrm{o}}^{(\mathrm{tx})}$, of such an OFDM transmitter is

$$M_{\mathrm{o}}^{(\mathrm{tx})} = \frac{N}{2}\log_2 N \tag{17}$$

and the number of complex additions, $A_{\mathrm{o}}^{(\mathrm{tx})}$, is

$$A_{\mathrm{o}}^{(\mathrm{tx})} = N\log_2 N \tag{18}$$

The TP-FDM transmitter replaces the N-point IFFT of OFDM with k smaller N/k-point IFFTs. Hence, the total number of complex multiplications in our scheme is

$$M_{\mathrm{tp}}^{(\mathrm{tx})} = k\left(\frac{N}{2k}\log_2\left(\frac{N}{k}\right)\right) = \frac{N}{2}(\log_2 N - \log_2 k) \tag{19}$$

and the total number of additions is

$$A_{\mathrm{tp}}^{(\mathrm{tx})} = k\left(\frac{N}{k}\log_2\left(\frac{N}{k}\right)\right) = N(\log_2 N - \log_2 k) \tag{20}$$

We thus have, at the transmitter, reduced the number of multiplications by

$$M_{\mathrm{o}}^{(\mathrm{tx})} - M_{\mathrm{tp}}^{(\mathrm{tx})} = \frac{N}{2}\log_2 k \tag{21}$$

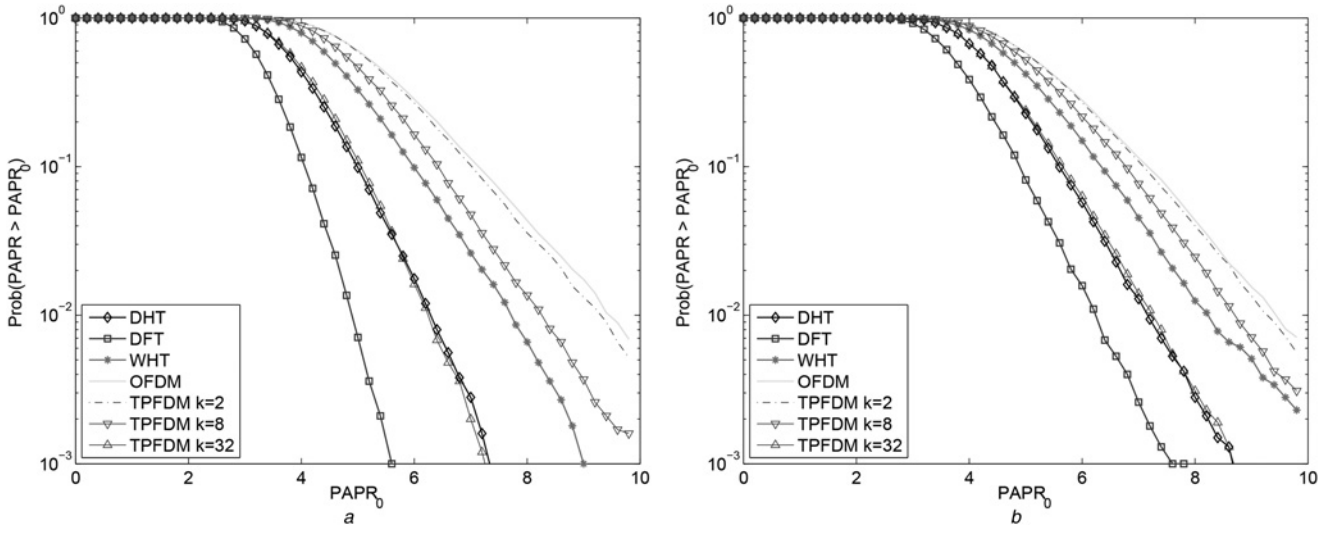

Fig. 3 *CCDF of PAPR*
a QPSK modulation
b QAM64 modulation

IET Commun., 2015, Vol. 9, Iss. 12, pp. 1450–1457

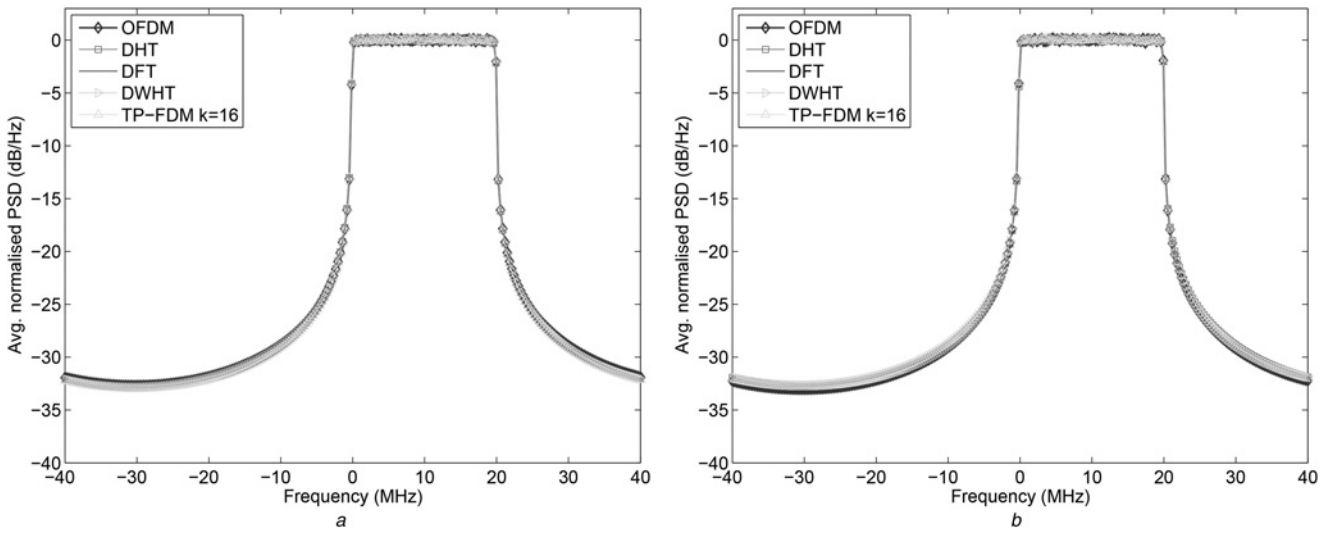

Fig. 4 *Averaged PSD for various schemes*

a QPSK modulation
b QAM-64 modulation

and the number of additions by

$$A_{\mathrm{o}}^{(\mathrm{tx})} - A_{\mathrm{tp}}^{(\mathrm{tx})} = N \log_2 k \tag{22}$$

At the receiver, there is an increase in computation compared to OFDM. We use similar notation for the number of complex multiplications and additions at the receivers of OFDM and TP-FDM as that for the transmitters, except that we replace the superscript (tx) with (rx). The additional block involves N/k different k-point FFT operations (step 2) and N multiplications (step 4). The excess number of complex multiplications and additions at the receiver compared to the receiver of conventional OFDM are hence

$$M_{\mathrm{tp}}^{(\mathrm{rx})} - M_{\mathrm{o}}^{(\mathrm{rx})} = \frac{N}{k}\left(\frac{k}{2}\log_2 k\right) + N = \frac{N}{k}\left(k + \frac{k}{2}\log_2 k\right) \tag{23}$$

and

$$A_{\mathrm{tp}}^{(\mathrm{rx})} - A_{\mathrm{o}}^{(\mathrm{rx})} = N \log_2 k \tag{24}$$

From (21) and (23), we see that TP-FDM has a total net (sum at both transmitter and receiver) increase in complex multiplications of N compared to OFDM. From (21) and (23), we observe that there is no net change in the number of additions between TP-FDM and OFDM. Effectively, the number of excess multiplications is $O(N)$, whereas the total multiplications of both conventional OFDM and our scheme (transmission plus reception) is $O(N\log_2 N)$. Note that in our analysis, we have counted trivial multiplications by 1. Ignoring these, the net increase in complex multiplications can, in fact, be shown to be less than N.

4.3 Power spectral density (PSD)

In this section we study the PSD of baseband signals of TP-FDM and other transform precoded OFDM signals. In Figs. 4*a* and *b*, we have plotted the average PSD against frequency for the 20 MHz wide signals used in simulations in Section 5.3.2. The averaging was performed over a thousand randomly generated realisations. We have also smoothened the PSD plots by averaging four consecutive frequency bins of the PSD plot. This effectively removes the ripples of the sinc-like pattern in the PSD which makes visual comparison of the PSD plots difficult.

Observe from Figs. 4*a* and *b* that the PSD plots of the DHT-precoded OFDM, WHT-precoded OFDM, DFT-precoded OFDM and OFDM are almost the same as that of TP-FDM (for $k = 16$). The PSD for TP-FDM varies very little with k and are hence omitted.

5 Extension to the multi-user case

In multi-user access systems (such as uplink in LTE), several users share the available subcarriers and transmit simultaneously to a central node (such as a basestation). Suppose that there are L users, each is assigned N subcarriers, and that the total number of subcarriers is $M = NL$. If each user employs OFDMA, then it maps data symbols on N subcarriers, zeroes out other subcarriers, and then proceeds with an IFFT, cyclic prefix, and other operations of OFDM. To reduce the high PAPR, users in LTE instead employ SC-FDMA, which is single carrier modulation applied to an FDMA system [6].

5.1 SC-FDMA

The block diagram for a baseband implementation of an SC-FDMA transmitter is shown in Fig. 5*a*. Instead of feeding the data symbols directly to the length-M IFFT block of OFDMA, first an N-point FFT is applied to it. The resultant N-point signal is mapped to N subcarriers and the rest set to zero through a subcarrier map. The mapping can be localised or distributed (interleaved). In localised mapping, all N subcarriers carrying data are clubbed together, whereas in interleaved mapping (called IFDMA) only every Lth subcarrier carries data. Interleaved subcarrier mapping has been shown to have better PAPR than localised mapping [7]. After this, normal OFDM operations are carried out.

The receiver consists of a normal OFDM receiver with an additional subcarrier demapping block and an N-point FFT block towards the end of the chain (see Fig. 5*b*).

5.2 TP-FDMA

Extending our scheme, described for two-user communication hitherto, to multi-user FDMA systems is straightforward. We call our scheme for multi-user communications TP-FDMA.

5.2.1 Transmitter structure: The TP-FDMA transmitter block diagram is depicted in Fig. 6*a*. The transmitter first performs the

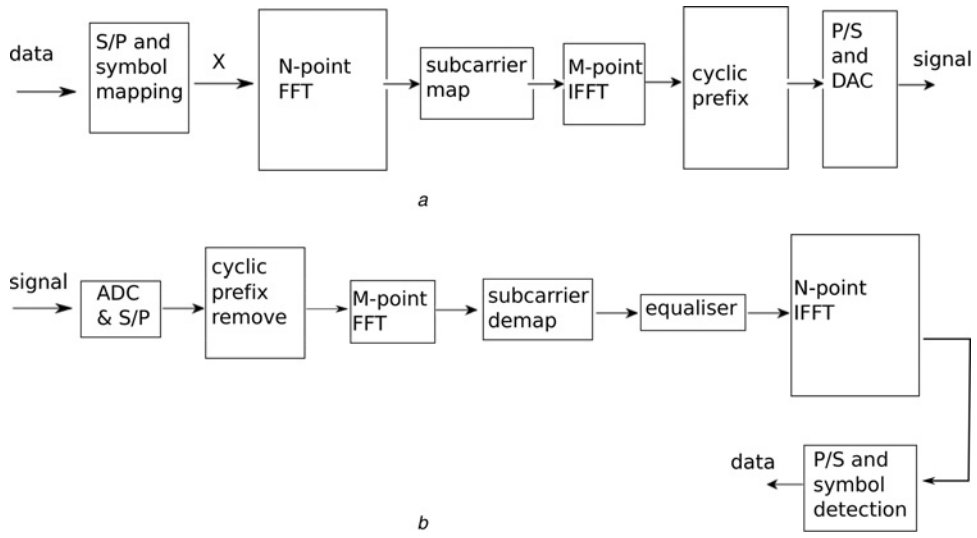

Fig. 5 *SC-FDMA block diagrams*

a SC-FDMA transmitter
b SC-FDMA receiver

following matrix operations on the input symbol vector $\boldsymbol{X}$ to generate the input $\boldsymbol{Q}$ to the subcarrier map block

$$\boldsymbol{Q} = \boldsymbol{P}_k \boldsymbol{B}_k \boldsymbol{P}_{N/k} \boldsymbol{D}_{N/k} \boldsymbol{X} \tag{25}$$

From (7), observe that the product $\boldsymbol{P}_k \boldsymbol{B}_k \boldsymbol{P}_{N/k} \boldsymbol{D}_{N/k}$ is in fact a partial implementation of an N-point FFT. The rest of the transmitter chain from the subcarrier map onwards is identical to that of the SC-FDMA transmitter.

TP-FDMA reduces to OFDMA and SC-FDMA for special choices of parameter k. For the special case of $k = 1$ we have

$$\boldsymbol{Q} = \boldsymbol{P}_1 \boldsymbol{B}_1 \boldsymbol{P}_N \boldsymbol{D}_N \boldsymbol{X} = \boldsymbol{X} \tag{26}$$

which corresponds to OFDMA, and for the case $k = N$ we have

$$\boldsymbol{Q} = \boldsymbol{P}_N \boldsymbol{B}_N \boldsymbol{P}_1 \boldsymbol{D}_1 \boldsymbol{X} = \boldsymbol{G}_N \boldsymbol{X} \tag{27}$$

which corresponds to SC-FDMA.

We note that in the case when $N = M$, the multi-user case reduces to a single-user scenario and TP-FDMA reduces to TP-FDM. To prove this, consider the TP-FDMA time domain signal prior to addition of the cyclic prefix

$$\begin{aligned} \boldsymbol{G}_M^{\mathrm{H}} \boldsymbol{Q} &= \boldsymbol{G}_N^{\mathrm{H}} \boldsymbol{Q} \\ &= \boldsymbol{P}_{N/k} \boldsymbol{B}_{N/k}^{\mathrm{H}} \boldsymbol{D}_{N/k}^{\mathrm{H}} \boldsymbol{P}_k \boldsymbol{B}_k^{\mathrm{H}} \boldsymbol{P}_{N/k} \boldsymbol{P}_k \boldsymbol{B}_k \boldsymbol{P}_{N/k} \boldsymbol{D}_{N/k} \boldsymbol{X} \\ &= \boldsymbol{P}_{N/k} \boldsymbol{B}_{N/k}^{\mathrm{H}} \boldsymbol{X} \end{aligned} \tag{28}$$

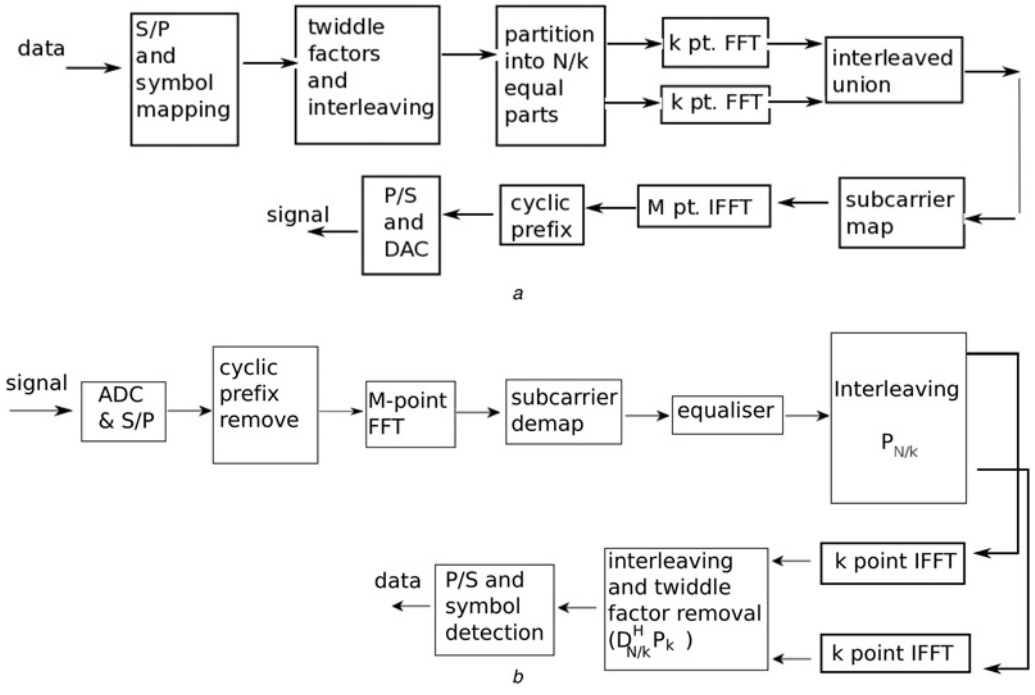

Fig. 6 *TP-FDMA block diagrams*

a TP-FDMA transmitter
b TP-FDMA receiver

IET Commun., 2015, Vol. 9, Iss. 12, pp. 1450–1457

This signal is identical to the TP-FDM time-domain signal y given by (9).

5.2.2 Receiver structure: The TP-FDMA receiver structure is depicted in Fig. 6*b*. It is identical to the SC-FDMA receiver structure till the equaliser block. Following equalisation, the TP-FDMA receiver performs the matrix multiplication $\boldsymbol{D}_{N/k}^{\mathrm{H}}\boldsymbol{P}_k\boldsymbol{B}_k^{\mathrm{H}}\boldsymbol{P}_{N/k}$ which inverts the operations at the transmitter.

Remark: The transmitter structure of TP-FDMA can be further optimised for efficiency by excluding the product $\boldsymbol{P}_{N/k}\boldsymbol{D}_{N/k}$ in (25). In this case, the receiver must also exclude the product $\boldsymbol{D}_{N/k}^{\mathrm{H}}\boldsymbol{P}_k$.

5.3 Performance analysis of TP-FDMA

We now study the performance of TP-FDMA in terms of PAPR, symbol decodability and SER.

5.3.1 PAPR analysis of TP-FDMA: In this section, we analyse the PAPR of TP-FDMA in the distributed subcarrier mapping case. It has been shown that the SC-FDMA transmitted signal (with distributed carrier mapping), also called interleaved-FDMA (IFDMA), in the time domain is just a periodic repetition (L times repetition) of the input constellation points $\boldsymbol{X}$ [7, 25]. Thus, IFDMA has the same PAPR as the input constellation vector. If all constellation points have the same power, then the PAPR of the IFDMA time-domain signal is 1. We use this fact in proving the following theorem.

Theorem 3: TP-FDMA with distributed subcarrier mapping has a PAPR of N/k.

Proof: We first prove that giving the following vector q as input symbol vector to the SC-FDMA transmitter chain

$$\boldsymbol{q} = \boldsymbol{P}_{N/k}\boldsymbol{B}_{N/k}^{\mathrm{H}}\boldsymbol{X} \tag{29}$$

results in the TP-FDMA signal. The input to the subcarrier map block then becomes

$$\begin{aligned}\boldsymbol{G}_N q &= \boldsymbol{P}_k\boldsymbol{B}_k\boldsymbol{P}_{N/k}\boldsymbol{D}_{N/k}\boldsymbol{B}_{N/k}\boldsymbol{P}_k\boldsymbol{P}_{N/k}\boldsymbol{B}_{N/k}^{\mathrm{H}}\boldsymbol{X}\\ &= \boldsymbol{P}_k\boldsymbol{B}_k\boldsymbol{P}_{N/k}\boldsymbol{D}_{N/k}\boldsymbol{X}\end{aligned} \tag{30}$$

which is identical to Q, the input to the subcarrier block of TP-FDMA [see (25)].

Thus, an SC-FDMA transmitter with a pre-processing step given by (29) generates the TP-FDMA signal. Consequently, with distributed subcarrier mapping, the TP-FDMA signal is identical to that of IFDMA with the same pre-processing step. Since IFDMA has the same PAPR as its input constellation vector, it follows that the PAPR of the TP-FDMA signal is the same as the PAPR of $\boldsymbol{q}$ in (29).

Comparing (29) and (9), we see that $\boldsymbol{q}$ is identical to the TP-FDM signal y, which itself has PAPR N/k. Hence TP-FDMA with distributed subcarrier mapping has a PAPR of N/k. □

5.3.2 SER performance of TP-FDMA: Recall that any TP-FDMA subcarrier is mapped to an element of Q or 0. Comparing (16) and (25), we see that the TP-FDMA non-zero subcarriers are identical to those of TP-FDM in the frequency domain. Thus, for the AWGN channel model and for a channel model in which each subcarrier faces i.i.d. fading (e.g. i.i.d. Rayleigh fading), the SER performance analysis of TP-FDMA is identical to that of TP-FDM.

6 Conclusion and discussion

We have presented TP-FDM, a frequency division multiplexing scheme with tunable PAPR, which has OFDM and SC modulation as special cases. While SC modulation gives smaller PAPR than OFDM, it performs worse than OFDM in terms of SER for Rayleigh fading channels. TP-FDM is flexible enough to allow one to trade-off PAPR with SER with the help of a parameter k. Thus, instead of choosing one of either extreme, OFDM or SC modulation, as is currently done in some cellular systems, one can choose the parameter k to tune the PAPR to the maximum suitable for the transmitter and receiver device electronics, so as to minimise the SER.

Analysis of TP-FDM performance for other channel models and in the presence of intercarrier interference (ICI) because of the Doppler effect and phase noise are potential avenues for future research. It has been shown that reduction of PAPR in the time domain for SC-FDMA when compared to OFDMA can result in larger instantaneous ICI in the former [26]. Since SC-FDMA and OFDMA are special cases of TP-FDMA, we speculate that this tradeoff between PAPR and ICI will also manifest itself in TP-FDMA.

7 References

1 Jiang, T., Wu, Y.: 'An overview: peak-to-average power ratio reduction techniques for OFDM signals', *IEEE Trans. Broadcast.*, 2008, **54**, (2), pp. 257–268
2 Molisch, A.F.: 'Wireless communications' (Wiley, 2010)
3 Wunder, G., Fischer, R.F.H., Boche, H., Litsyn, S., No, J.-S.: 'The PAPR problem in OFDM transmission: new directions for a long-lasting problem', *IEEE Signal Process. Mag.*, 2013, **30**, (6), pp. 130–144
4 Ouyang, X., Jin, J., Jin, G., Wang, Z.: 'Low complexity discrete Hartley transform precoded OFDM for peak power reduction', *Electron. Lett.*, 2012, **48**, (2), pp. 90–91
5 Ahmed, M.S., Boussakta, S., Sharif, B.S., Tsimenidis, C.C.: 'OFDM based on low complexity transform to increase multipath resilience and reduce PAPR', *IEEE Trans. Signal Process.*, 2011, **59**, (12), pp. 5994–6007
6 'Single Carrier FDMA in LTE', White Paper by IXIACOM, http://www.ixiacom.com/sites/default/files/resources/whitepaper/SC-FDMA-INDD.pdf, accessed November 2014
7 Myung, H., Lim, J., Goodman, D.: 'Single carrier FDMA for uplink wireless transmission', *IEEE Veh. Technol. Mag.*, 2006, **1**, (3), pp. 30–38
8 Priyanto, B.E., Codina, H., Rene, S., Sorensen, T., Mogensen, P.: 'Initial performance evaluation of DFT-spread OFDM based SC-FDMA for UTRA LTE uplink'. Proc. Vehicular Technology Conf. VTC2007, Spring, Dublin, Ireland, April 2007, pp. 3175–3179
9 Ren, G., Zhang, H., Chang, Y.: 'A complementary clipping transform technique for the reduction of peak-to-average power ratio of ofdm system', *IEEE Trans. Consumer Electron.*, 2003, **49**, (4), pp. 922–926
10 Ju, S., Leung, S.: 'Clipping on COFDM with phase on demand', *IEEE Commun. Lett.*, 2003, **7**, (2), pp. 49–51
11 O'neill, R., Lopes, L.: 'Envelope variations and spectral splatter in clipped multicarrier signals'. Proc. Personal, Indoor and Mobile Radio Communications, 1995, pp. 71–75
12 Ochiai, H., Imai, H.: 'Performance analysis of deliberately clipped OFDM signals', *IEEE Trans. Commun.*, 2002, **50**, (1), pp. 89–101
13 Yang, K., Chang, S.-I.: 'Peak-to-average power control in OFDM using standard arrays of linear block codes', *IEEE Commun. Lett.*, 2003, **7**, (4), pp. 174–176
14 Slimane, S.B.: 'Reducing the peak-to-average power ratio of OFDM signals through precoding', *IEEE Trans. Veh. Technol.*, 2007, **56**, (2), pp. 686–695
15 Ginige, T., Rajatheva, N., Ahmed, K.M.: 'Dynamic spreading code selection method for PAPR reduction in OFDM-CDMA systems with 4-QAM modulation', *IEEE Commun. Lett.*, 2001, **5**, (10), pp. 408–410
16 Muller, S.H., Huber, J.B.: 'OFDM with reduced peak-to-average power ratio by optimum combination of partial transmit sequences', *Electron. Lett.*, 1997, **33**, (5), pp. 368–369
17 Zhou, G., Baxley, R., Chen, N.: 'Selected mapping with monomial phase rotations for peak-to-average power ratio reduction in OFDM'. Proc. Communications, Circuits and Systems ICCCAS 2004, Chengdu, China, June 2004, pp. 66–70
18 Sharif, M., Hassibi, B.: 'Existence of codes with constant PMEPR and related design', *IEEE Trans. Signal Process.*, 2004, **52**, (10), pp. 2836–2846
19 Sharif, M., Tarokh, V., Hassibi, B.: 'Peak power reduction of OFDM signals with sign adjustment', *IEEE Trans. Commun.*, 2009, **57**, (7), pp. 2160–2166
20 Wang, X., Tjhung, T., Ng, C.: 'Reduction of peak-to-average power ratio of OFDM system using a companding technique', *IEEE Trans. Broadcast.*, 1999, **45**, (3), pp. 303–307
21 Yoo, S., Yoon, S., Kim, S.Y., Song, I.: 'A novel PAPR reduction scheme for OFDM systems: selective mapping of partial tones (SMOPT)', *IEEE Trans. Consumer Electron.*, 2006, **52**, (1), pp. 40–43
22 Krishnamoorthi, R.: 'Partial FFT processing and demodulation for a system with multiple subcarriers'. US Patent 7720162, May 2010
23 Proakis, J.G., Manolakis, D.K.: 'Digital signal processing: principles, algorithms, and applications, 4/e' (Pearson Education India, 2007)
24 Baig, I., Jeoti, V.: 'PAPR analysis of DHT-precoded OFDM system for M-QAM'. Proc. Int. Conf. on Intelligent and Advanced Systems (ICIAS), June 2010, pp. 1–4
25 Sorger, U., De Broeck, I., Schnell, M.: 'Interleaved FDMA-a new spread-spectrum multiple-access scheme'. Proc. IEEE Int. Conf. on Communications, June 1998, pp. 1013–1017
26 Choi, Y.-S., Yang, R., Wang, J., Harel, T., Lomnitz, Y., Yin, H.: 'On the multiple access schemes for IEEE 802.16m: comparison of SC-FDMA and OFDMA'. Presentation by Intel at TGm Call for contribution on SDD, January 2008, http://www.ieee802.org/16/tgm/contrib/C80216m-08_045r1.ppt, Document Number: C802.16m-08/045r1, accessed February 2015